This article was downloaded by:
On: *26 January 2011*
Access details: *Access Details: Free Access*
Publisher *Taylor & Francis*
Informa Ltd Registered in England and Wales Registered Number: 1072954 Registered office: Mortimer House, 37-41 Mortimer Street, London W1T 3JH, UK

Liquid Crystals
Publication details, including instructions for authors and subscription information:
http://www.informaworld.com/smpp/title~content=t713926090

Polymer dispersed liquid crystals: relation between formulation, electro-optical properties and morphology

C. Grand; M. F. Achard; F. Hardouin

Online publication date: 29 June 2010

To cite this Article Grand, C. , Achard, M. F. and Hardouin, F.(1997) 'Polymer dispersed liquid crystals: relation between formulation, electro-optical properties and morphology', Liquid Crystals, 22: 3, 287 — 296
To link to this Article: DOI: 10.1080/026782997209342
URL: http://dx.doi.org/10.1080/026782997209342

PLEASE SCROLL DOWN FOR ARTICLE

Full terms and conditions of use: http://www.informaworld.com/terms-and-conditions-of-access.pdf

This article may be used for research, teaching and private study purposes. Any substantial or systematic reproduction, re-distribution, re-selling, loan or sub-licensing, systematic supply or distribution in any form to anyone is expressly forbidden.

The publisher does not give any warranty express or implied or make any representation that the contents will be complete or accurate or up to date. The accuracy of any instructions, formulae and drug doses should be independently verified with primary sources. The publisher shall not be liable for any loss, actions, claims, proceedings, demand or costs or damages whatsoever or howsoever caused arising directly or indirectly in connection with or arising out of the use of this material.

LIQUID CRYSTALS, 1997, VOL. 22, NO. 3, 287–296

Polymer dispersed liquid crystals: relation between formulation, electro-optical properties and morphology

by C. GRAND, M. F. ACHARD and F. HARDOUIN*
Centre de Recherche Paul Pascal/C.N.R.S., Université Bordeaux I,
Avenue Albert Schweitzer, F-33600 Pessac, France

(*Received 28 July 1996; accepted 18 October 1996*)

Polymer Dispersed Liquid Crystal (PDLC) films investigated in this work are obtained by phase separation induced by photopolymerization of a homogeneous 'prepolymer/liquid crystal' mixture. We show a close relation between the formulation/conditions of preparation of the materials, their morphology and their electro-optical properties. The effect of the mutual compatibility of the prepolymer and the liquid crystal on film performances is investigated using 'model systems' that consist of pure components. Finally, both SALS experiments and a Fourier Transform procedure lead to a simple model in which LC domains are separated by polymer walls.

Downloaded At: 08:31 26 January 2011

1. Introduction

Over the last decade a wide variety of polymer/liquid crystal composites has been studied for their numerous potential applications [1], in particular windows and devices operating on the principle of electrically controlled light scattering. Among these composites, PDLC films consist of liquid crystal domains dispersed in a polymer matrix [2]. They can be prepared by a phase separation process induced either by cooling a homogeneous mixture of polymer and low molecular mass liquid crystal (LC) (Thermally Induced Phase Separation, TIPS) or by evaporating a solvent from a polymer/LC solution (Solvent Induced Phase Separation, SIPS), or by polymerization of homogeneous initial mixture of monomer and LC (Polymerization Induced Phase Separation, PIPS).

The polymerization induced phase separation is a widely used method of PDLC formation: as the reaction of polymerization proceeds, the LC gradually becomes less soluble in the forming polymer, causing the initial homogeneous solution to separate into two phases, an LC-rich phase and an isotropic polymer-rich phase. The conditions under which the materials are obtained will give rise to different properties of the resulting PDLC. In this work, we will investigate the parameters which influence the phase separation process, induced by photopolymerization under UV light, to control the characteristics of the final material. To this aim, we will first focus on the formulation of the initial solution of prepolymer (polymerizable monomers and oligomers) and liquid crystal. Then, we will describe the effect of different curing parameters such as temperature or the nature and the proportion of the crosslinking agent on the electro-optical performances of the PDLC. In addition, the morphology of the films will be systematically investigated. Finally, we will try to establish a triangular relation between the formulation/conditions of preparation of the materials, their morphology and their electro-optical properties [3].

*Author for correspondence

2. Experimental

2.1. *Sample preparation*

Many of the early publications on PDLC using nematic liquid crystals refer to the use of cyanobiphenyl mixtures. In this study, we first employ 4-pentyl-4′-cyanobiphenyl (5CB) and then a high birefringence nematic mixture specifically designed for PDLC applications (TL205 purchased from Merck Ltd).

The polymer matrix is made from (a) monofunctional acrylate monomers and oligomers such as isodecyl acrylate (IDA), 2-hydroxyethyl acrylate (2-HEA), 2-ethylhexyl acrylate (2-EHA), pentadecafluoro-octyl acrylate (PDFA), polybutadiene (1,4) acrylate (PBA)†, and (b) multifunctional acrylate monomers and oligomers such as polyethylene glycol 400 diacrylate (PEG400), polybutandiol diacrylate (PBDD)‡, pentaerythritol triacrylate (PETA) and dipentaerythritol pentaacrylate (DPEPA). The initial mixture of the monomers

† $CH_2=CHCOO\ (CH_2-CH=CH-CH_2)_{240}H$
$M=2260\,g\,mol^{-1}$.

‡ $CH_2=CHCOO\ (CH_2-CH_2-CH_2-CH_2-O-)_{27}OC-CH=CH2$
$M=2000\,g\,mol^{-1}$.

0267–8292/97 $12·00 © 1997 Taylor & Francis Ltd.

and oligomer precursors of the final polymer is referred to as 'prepolymer'.

The photoinitiators employed are Darocur 1173 and Darocur 4265 from Ciba-Geigy.

The liquid crystal, the prepolymer and the photoinitiator are mixed at room temperature and vigorously stirred until a homogeneous, clear mixture is obtained. This mixture is then introduced by capillary action into an electro-optic cell composed of two indium/tin oxide coated glass plates with 8 μm or 14 μm spacers.

The photopolymerization is carried out by irradiating the cells under UV light from a mercury lamp (Tecklite-ELC 4000). The UV intensity is usually 15 mW cm^{-2} and the irradiation time 10 minutes. The curing temperature T is controlled by using both an IR filter (water cooled) between the lamp and the sample, and a hot stage containing the sample coupled to a thermostat (Haake F3).

2.2. *Mesomorphic characterization and electro-optical measurements*

The composition of the liquid crystalline phase in the PDLC is usually different from that of the initial LC mixture: some components of the prepolymer can remain dissolved in the liquid crystalline phase and some constituent(s) of the liquid crystal in the polymer. Thus the 'quality' of the phase separation process is evaluated through the determination of the isotropic–nematic transition temperature of the LC-rich phase of the PDLC. This temperature obtained either by microscopic observation (Leitz microscope and Mettler FP52 hot stage) or by Differential Scanning Calorimetry (Perkin Elmer DSC7) is compared with that of the pure liquid crystal.

For electro-optic measurements, the collimated beam of He/Ne laser (wavelength of 632·8 nm) is passed through the cell, normal to the film surface and the transmitted light is collected by a luminance meter (Topcon BM8) with a 0·2° collection angle. Using a function generator (Wavetech), an electric field is applied across the samples (50 Hz square wave). The voltage–transmission curves are thus measured. Four characteristic parameters are usually determined: V_{10} (respectively V_{90}) represents the voltage corresponding to 10% (90%) of light transmitted and T_{OFF} (T_{ON}) the percentage of light transmitted in the OFF and the ON state. The contrast is usually defined as the ratio T_{ON}/T_{OFF}.

2.3. *Film morphology analysis*

The morphology of a PDLC can considerably vary depending on both the formulation and the conditions of preparation. In this sense, a quantitative evaluation of the morphology is of great interest in characterizing the material. With this aim, two techniques are used: a normal small angle light scattering technique and a more original image analysis.

For the small angle light scattering experiments, a classical set-up with a Krypton laser (647 nm) is used. Scattering of laser light by the samples is recorded via a video camera. Images are then digitalized using an imaging system (Pericolor 2001) and finally transferred to a computer. The amplitude profile $A(q)$, where q is the scattering wave vector, is then extracted from the diffraction patterns. The main aim of this morphological investigation is to find a suitable fit to the amplitude profiles $A(q)$ which should lead to a characteristic size for the sample.

The second method that we used for studying these morphologies consists in a numerical treatment of microscopic images of the films obtained by direct microscopic observations (Leitz microscope). Images are recorded on video by a camera and digitalized. At this stage, numerical images, typically 512×512 pixels size, are processed by computing their 2-dimensional discrete Fourier Transform by means of a classical Fast Fourier Transform (FFT) algorithm [4]. With this processing, we obtain the 2D spatial frequency spectrum of the PDLC films, which is qualitatively equivalent to the diffraction patterns obtained by direct light scattering experiments. For both techniques, a hot stage (Mettler FP52) is used to control the temperature of the samples. Indeed, two types of characterization have been performed, depending on the state of the LC-rich phase of the PDLC, nematic or isotropic. Nematic state experiments are carried out at room temperature, and isotropic state experiments at a temperature higher than the isotropic–nematic temperature of the pure liquid crystal.

First, SALS experiments performed on 'nematic state' PDLC between crossed polarizers give diffraction patterns which look like a 'four leafed clover' (figure 1). Qualitatively, comparison with direct microscopic observations shows that the larger the leaves are, the smaller the nematic domains. Similar results have been found in previous experiments on crystalline [5] or mesomorphic [6] polymers. For a more quantitative viewpoint, a SALS theory based on the Rayleigh–Gans approximation has been developed [7] to determine the size of the spherulites formed during the polymer growth from the 'four leafed clover' pattern. More recently, an attempt has been made to expand it to the measurement of the size of the nematic droplets of the PDLC in respect of their configuration, radial and axial [8] or bipolar [9]. Nevertheless, none of the relations given by these authors allowed us to determine the accurate droplet size. In all cases, sizes given by such a procedure were overestimated compared with microscopic observations.

We therefore tried to investigate these 'nematic state' PDLC films by means of the FT procedure. As in

Downloaded At: 08:31 26 January 2011

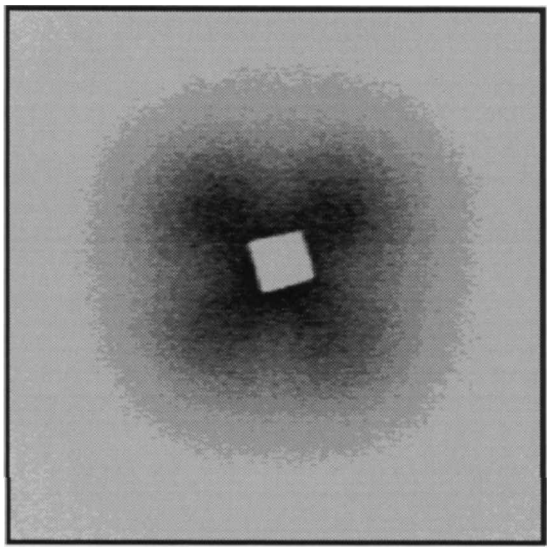

Figure 1. SALS diffraction pattern of a PDLC film at room temperature: the LC domains are in the nematic state (SALS-crossed polarizers).

Downloaded At: 08:31 26 January 2011

previous experiments, crossed polarizers were used and samples were at room temperature. Figure 2 (a) shows an example of the image obtained by microscopic observation. The corresponding diffraction patterns obtained by FT are disc-shaped (figure 2 (*b*)) and we do not observe 'four leafed clover' patterns as previously. We attribute this difference to the fact that the real space image taken by the camera is only sensitive to interfaces, and thus the image analysis does not take into account the orientation fluctuation of the nematic director inside the droplet. However, it should be noted that, as in the case of SALS experiments, smaller nematic domains lead to larger diffraction pattern sizes. To find out a characteristic size from these image analysis data, we first assume that nematic domains are quite similar to discs. Moreover, since no structure between droplets could be observed, the structure factor $S(q)$ is supposed to be equal to 1. The experimental amplitude profiles $A(q)$ are thus fitted using the form factor $F(q)$ of an homogeneous disc of radius a,

$$A(q) = F(q) = \int_0^a \int_0^{2p} \exp(\mathrm{i}qr\cos q) r \mathrm{d}r \mathrm{d}q \qquad (1)$$

In the 'Guinier' range ($qa \ll 1$), equation (1) becomes the equivalent two-dimension Guinier's law [10].

$$A(q)_{q\to 0} = A(0)\exp\left(-\frac{a^2}{8}q^2\right) \qquad (2)$$

Therefore the average radius of the LC droplet, a, is expected to be given by the fits to the experimental curves $A(q)$ with equation (2). Figure 2 (*c*) shows that, in

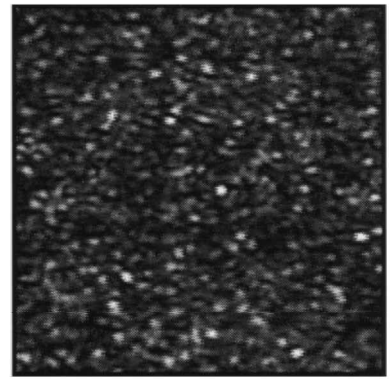

(*a*)

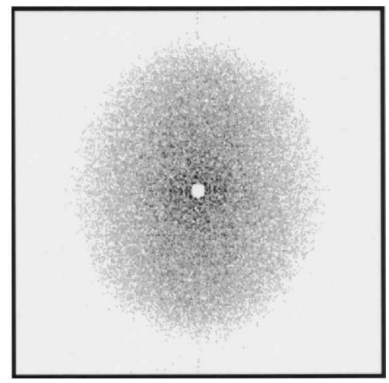

(*b*)

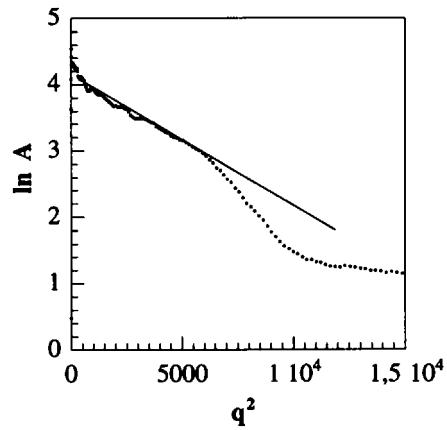

(*c*)

Figure 2. (*a*) Real space microscopic image of a PDLC film in the 'nematic state' (crossed polarizers; 0·6 μm is represented by 1 mm). (*b*) Diffraction pattern obtained by FT procedure corresponding to the real space microscopic image of figure 2 (*a*). (*c*) Evolution of $\ln A = f(q^2)$ corresponding to the FT diffraction pattern.

agreement with equation (2), $\ln A(q) = f(q^2)$ experimental plots exhibit a linear behaviour in the limit of small q. Thus an average radius of droplet, a, can be directly determined from the slope of the straight line. The FT procedure seems therefore to provide a useful tool to

determine an average size of LC droplets, which is not easily accessible using SALS experiments. However, with this method, the resolution limit of the microscope prevents our measuring sizes below 1 μm.

In the 'isotropic PDLC experiments', samples are heated at a temperature at which the LC-rich phase inside the droplet is isotropic. In this state, we visualize by microscopic observations a regular network which may be due to the small difference between the isotropic refractive index n_i of the LC-rich phase and index n_p of polymer-rich phase (figure 3 *a*). At room temperature, this network is masked by the nematic birefringence. Noticing that the periodicity of this network was dependent on polymerization conditions, we tried to determine this new characteristic size by means of both SALS and FT experiments: the diffraction patterns are now similar. They exhibit a ring whose size changes with network periodicity d (figure 3 (*b*)). As a consequence, amplitude profiles $A(q)$ show a 'Bragg' peak (figure 3 (*c*)). A measurement of the wave vector q^{max} corresponding to the maximum in amplitude allows one to determine the network periodicity by:

$$d(\text{pixels}) = \frac{512}{q} \qquad \text{(FT procedure)}$$

$$d(\mu\text{m}) = \frac{2\pi}{q} \quad \text{with} \quad q = \frac{4\pi n}{\lambda} \sin\left(\frac{\theta}{2}\right) \qquad \text{(SALS)}$$

θ is the scattering angle and the index n of the 'isotropic state' films is assumed to be equal to 1·5. As we will see in the next section, quite similar values are found with both techniques and the small difference sometimes observed may be due to the approximation made in SALS experiments concerning the value of n.

To sum up, each type of experiment, 'nematic state' and 'isotropic state', provides us with a characteristic size of the films. We are able to measure an average LC droplet diameter, $2a$, by means of a numerical FT treatment of the real space image in the 'nematic state', and a polymer network periodicity, d, by both FT procedure and SALS experiments in the 'isotropic state'. We are now able to appreciate the influence of several parameters of formulation and preparation through the electro-optic and morphological characterizations of the resulting PDLC.

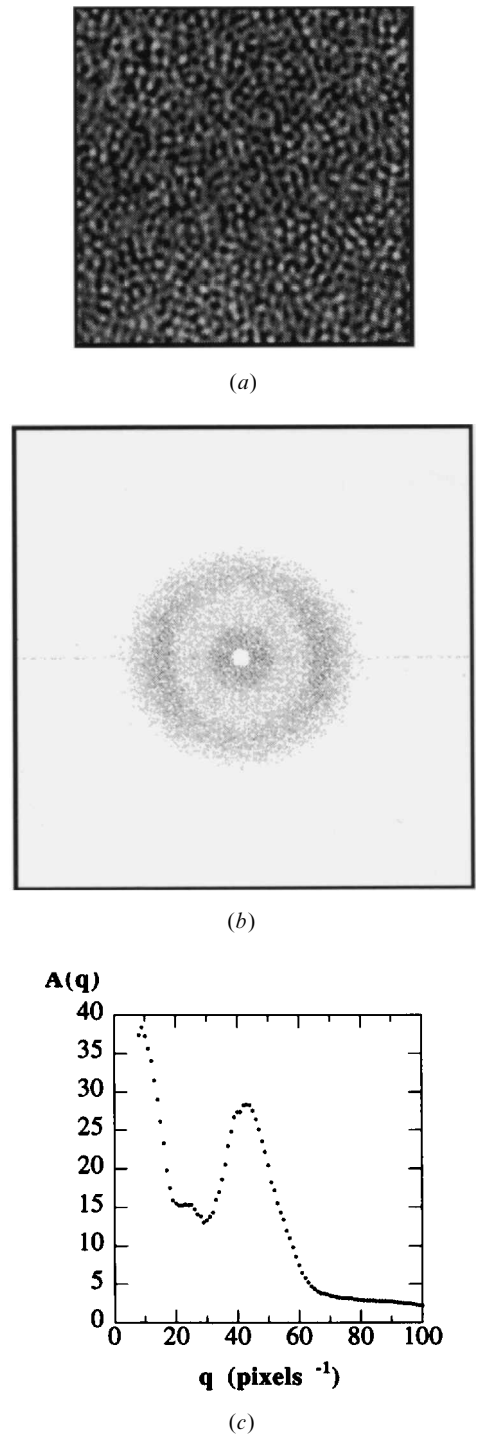

(*a*)

(*b*)

(*c*)

Figure 3. (*a*) Example of a real space microscopic image of a PDLC film in the 'isotropic state' (no polarizers; 1 μm is represented by 1 mm). (*b*) Diffraction pattern obtained by FT procedure or direct SALS experiment on films depicted in figure 3 (*a*). (*c*) Corresponding amplitude profile $A(q)$.

3. Results and discussion

3.1. *Formulation*

Our aim in this part is first to understand better the thermodynamic behaviour of different prepolymer/LC systems, and then, to formulate a UV-curable mixture that leads, after polymerization, to a PDLC with good electro-optical response. To achieve this, we focus on the mutual compatibility of the initial components, prepolymer and LC. Indeed, the liquid crystal and the prepolymer have to be sufficiently miscible to allow the desired amount of LC to dissolve and give a homogen-

Downloaded At: 08:31 26 January 2011

Downloaded At: 08:31 26 January 2011

eous LC/prepolymer mixture. In addition, the liquid crystal has to be sufficiently insoluble in the formed polymer; indeed it has been previously shown that depending on the initial formulation some uncured prepolymer remains dissolved in the LC-rich phase and that the polymer matrix contains a significant amount of LC [11, 12, 13]. It has also been suggested that the greater the solubility between prepolymer and LC, the larger the proportion of LC dissolved in the polymer matrix [11, 14]. In this sense the initial prepolymer/LC composition is of great importance.

To estimate the degree of compatibility of a prepolymer and a liquid crystal, the phase diagram of the prepolymer/LC system is investigated: on cooling down a homogeneous mixture containing a given weight fraction of LC, we determine the temperature T_S at which the initial isotropic mixture separates into a two-phase state, an isotropic phase I and a nematic phase N.

We first study 'model systems' for which both the LC and prepolymer are pure components. Phase diagrams of IDA/5CB, 2-HEA/5CB and PBA/5CB systems are reported in figure 4. Their topologies are qualitatively the same, but significant quantitative differences are observed. While the two components IDA and 5CB are miscible over a large range of temperature and concentration, it is worth noting the lower compatibility between the monomer 2-HEA and the liquid crystal 5CB and between the oligomer PBA and 5CB. In the case of PBA, this larger incompatibility is undoubtedly due to the difference in molar mass between this oligomer and the LC. However, this argument is not applicable in the case of 2-HEA, and we assume that the reason for the incompatibility between 2-HEA and 5CB is now enthalpic and that the incompatibility is enhanced by hydrogen bonds within the monomer, due to its hydroxyl group.

In addition, for a given liquid crystal concentration, it is possible to adjust the phase diagram of LC/prepolymer by choosing an appropriate formulation of the prepolymer: for example, as seen in figure 5, further addition of the oligomer PBA to IDA causes a

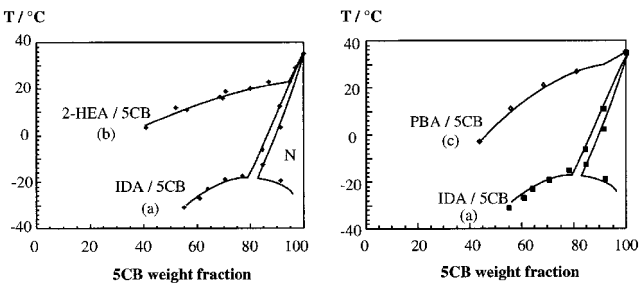

Figure 4. Phase diagrams before polymerization of the IDA/5CB (a), 2-HEA/5CB (b), and PBA/5CB (c) systems.

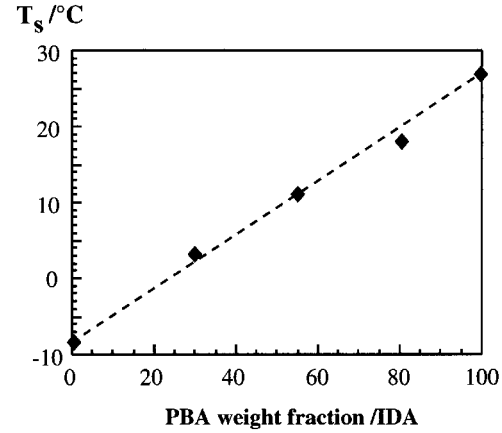

Figure 5. Linear dependence of phase separation temperature T_s on PBA weight fraction.

linear increase in T_s with oligomer weight fraction. Such a shift of the phase diagram with the oligomer fraction has already been reported [15]. A comparable increase of the incompatibility is also observed on adding 2-HEA or PDFA to IDA.

For a given liquid crystal, this optimization of the prepolymer formulation has to take into account the following conditions: the initial prepolymer/LC mixture is expected to be rich enough in LC (typically higher than 50 wt % LC) and must be homogeneous, if possible at room temperature to facilitate the experimental process. However, phase separation will be induced by polymerization only if the compatibility between the prepolymer and the LC (*a fortiori* between growing polymer and LC) is weak enough. Indeed, no phase separation has been observed on systems whose temperature T_s is very low with respect to curing temperature T. Thus, the starting point in the phase diagram before polymerization (corresponding to a given LC concentration and a given temperature) has to be taken into account to optimize the phase separation process. The initial LC concentration will be chosen close to the solubility limit of LC in the prepolymer at room temperature. Moreover, we noticed for all PDLC films studied that the isotropic–nematic transition temperature $T_{IN(PDLC)}$ of the LC-rich phase in the PDLC (i.e. after polymerization) increases with decreasing $(T\text{-}T_S)$. This indicates a better purity of the LC-rich phase of the film (i.e. less oligomer and prepolymer are dissolved in this phase) for PDLC samples cured at a temperature T close to T_s. This result suggests that the efficiency of the phase separation induced by the polymerization process strongly depends on the temperature and concentration of the initial prepolymer/LC mixture, and by these results on 'model systems' the notion of an 'LC/prepolymer optimum couple' is clearly advanced.

Results from 'model systems' have then been extrapol-

ated to the mesomorphic mixture TL205 optimized for electro-optical applications. We concentrated on the formulation of a prepolymer mixture 'best partner' of TL205. Several acrylate monomers have been tested with TL205 before polymerization. To avoid dealing with the whole phase diagram of all systems, we only studied mixtures containing 80 wt % of TL205. Phase separation temperatures T_S of those different systems are reported in table 1 and only two of the acrylates tested satisfy the condition of homogeneity at room temperature: 2-EHA and IDA.

For the following experiments, 2-EHA was chosen as the basic monomer and the phase diagram before polymerization of the 2-EHA/TL205 'couple' is reported in figure 6.

A final condition has to be taken into consideration in formulating the initial 'prepolymer/LC' mixture: the formulation of the prepolymer must contain a crosslinking compound to improve the scattering properties of the PDLC. Indeed, if a crosslinking compound is added, gelation occurs earlier, so that the droplets are trapped earlier and smaller droplets are formed. Four crosslinking monomers (with functionality essentially two or more) have been tested with the monomer 2-EHA: polyethyleneglycol 400 diacrylate (PEG400), polybutandiol diacrylate (PBDD), pentaerythritol triacrylate (PETA) and dipentaerythritol penta-acrylate (DPEPA). As shown in figure 7 the phase separation temperature T_S increases regularly with the mol fraction of crosslinking agent in the prepolymer. In the case of the PBDD/2-EHA and DPEPA/2-EHA systems, a biphasic region is observed at room temperature with less than 5 mol % of crosslinking agent. In order to investigate a large range of crosslinker proportions, the 'PEG400/2-EHA/TL205' and 'PETA/2-EHA/TL205' systems, which are in an isotropic one-phase state at room temperature even for large concentrations of crosslinking agent, were chosen. In the following, we therefore study PDLC films prepared from an optimized LC/prepolymer mixture composed of 80 wt % of TL205 and 20 wt % of '2-EHA/PEG400' or '2-EHA/PETA' prepolymer and containing 3 wt % of initiator in the prepolymer.

Table 1. Phase separation temperatures T_s of different '20 wt % prepolymer/80 wt % TL205' systems.

Prepolymer	T_s/°C
2-EHA	4
IDA	17
PBA	75
2-HEA	80
PDFA	>80

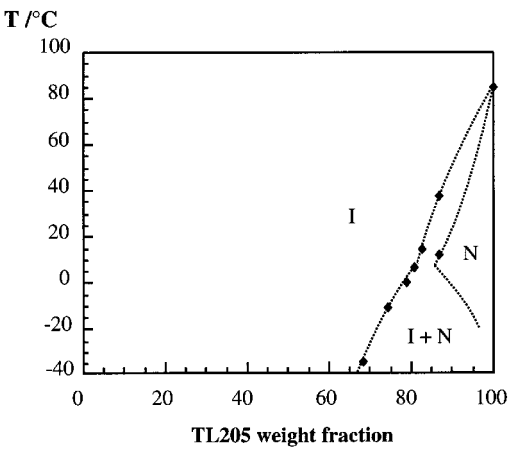

Figure 6. Phase diagram before polymerization of the 2-EHA/TL205 system.

3.2. *Electro-optical properties and morphology*

We were now able to characterize the films prepared with different formulations (crosslinking agent, initiator ...) and different curing temperatures and could try to identify a close link between the formulation, the electro-optical response and the morphology of the films.

Figure 8 shows the evolution with proportion of crosslinking agent of the voltage–transmission curves for (2-EHA/PEG400)/TL205 20:80 PDLC films. The most striking feature is the increase in both turbidity (lower off-state transmission T_{OFF}) and driving voltage with crosslinking agent rate. For display applications, PDLCs are expected to have not only high contrast, but also low driving voltage ($V < 10$ V). Therefore, a 'threshold rate' of crosslinking agent can be defined as the rate leading to the highest contrast for the lowest driving voltage. It can be seen in figures 9 and 10 that the 'threshold rate' for (2-EHA/PEG400)/TL205 (20:80) systems is about 4–5 mol % of PEG400 in the prepolymer. We should notice that the same 'threshold rate' was

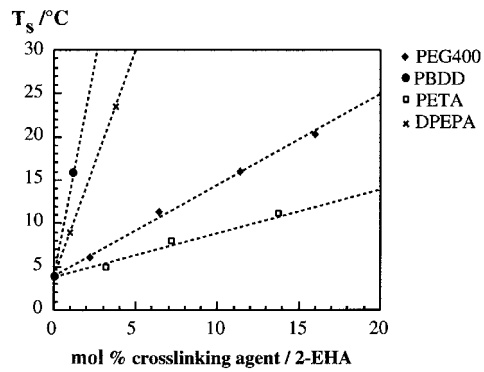

Figure 7. Mol fraction of crosslinking agent in the 2-EHA prepolymer versus phase separation temperature T_s. The mixtures contain 80 wt % of TL205.

Downloaded At: 08:31 26 January 2011

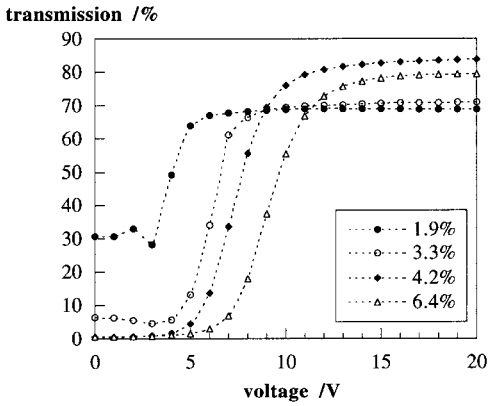

Figure 8. Voltage–transmission curves for different mol fractions of crosslinking agent in the prepolymer. (TL205/(2-EHA/PEG400) 80:20, Darocur 4265, $T = 20°C$, 15 mW cm^{-2}).

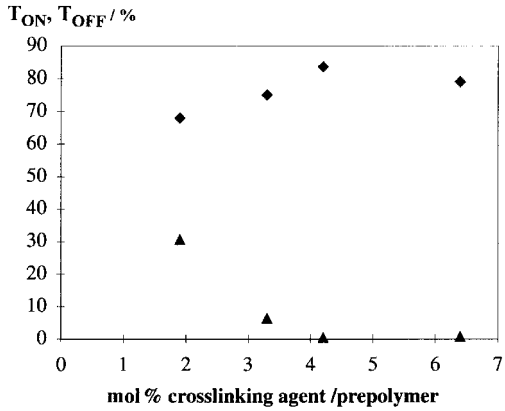

Figure 9. T_{OFF} and T_{ON} versus mol fraction of crosslinking agent in the prepolymer.

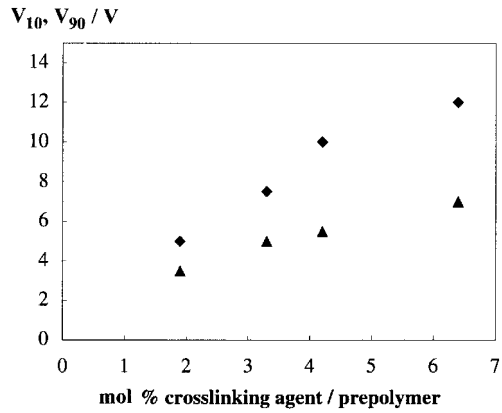

Figure 10. V_{10} and V_{90} voltages versus mol fraction of crosslinking agent in the prepolymer.

obtained for samples based on crosslinker PETA. Beyond this 'threshold rate', driving voltage goes on increasing, but no improvement in contrast can be seen.

Table 2 shows the network periodicity, d, and LC domain size, $2a$, for PDLC films prepared with increasing crosslinking agent concentration (PETA or PEG400). For all samples, the droplet diameter $2a$ was found to be smaller than the polymer network periodicity d. This therefore suggests a simple model where LC droplets are separated by thick polymer walls whose size is given by the value of $(d-2a)$. As expected, decrease of both network periodicity and LC domain size with increasing crosslinking agent rate is observed. Comparison of electro-optical results and morphology of the films clearly demonstrates a correlation between the size of the film structure and the electro-optical response. Morphology provides a particularly good explanation for the OFF-scattering state and driving voltage evolution. In fact, it seems that the optimum scattering state is observed when LC domain and polymer wall sizes become equal and close to the light wavelength ($(d-2a)$ compared to $2a$). Moreover, confinement of LC domains causing an increase in driving voltage is here evidenced.

Figure 11 shows the electro-optical curves of two films differing only by the nature of the initiator, Darocur 1173 or Darocur 4265. Stronger light scattering in the OFF state and higher driving voltage were observed for the PDLC film made from Darocur 4265, which is consistent with morphological analysis. Indeed, many and smaller structures were formed with Darocur 4265 (in this example, $d = 3{\cdot}9\,\mu m$ and $1{\cdot}9\,\mu m$ with, respectively, Darocur 1173 and Darocur 4265). We assumed that a more efficient initiation was carried out with the initiator Darocur 4265 and that this led to a faster polymerization process causing the medium to gel more quickly. As a consequence, the LC-rich domains trapped during the coalescing process were smaller. Finally, as in the case of higher concentration of crosslinking agent, a quicker polymerization/crosslinking process causes the medium to become more rapidly viscous, resulting in a thinner PDLC structure and therefore in both a low off-state transmission and a high driving voltage. Similar results were found in the case of a larger UV intensity [16].

The influence of the chemical nature of the crosslinking agent on electro-optical response is now illustrated in figure 12. While PDLC films prepared from PEG400 do not meet application requirements in terms of voltage, a film prepared from crosslinking agent PETA exhibits a higher contrast ratio and lower driving voltage. Contrary to previous results, it can be seen from the morphology size measurements that such an increase in voltage for PEG400 samples cannot here be assigned to smaller LC-rich domains (see table 2). On the contrary, LC confinement is more important on moving from PEG400 to PETA samples which are nevertheless prepared with the same curing parameters. Moreover, this shift towards lower voltage cannot be caused by a better

Downloaded At: 08:31 26 January 2011

Table 2. Network periodicity (d) and LC domain size ($2a$) for PDLC samples formed at 20°C with different crosslinking agent concentration. (=): size$<1\,\mu m$; V_{90}: voltage corresponding to 90% of transmitted light; T_{OFF}: percentage of transmitted light in the OFF state.

Cross linking agent		Light scattering	Image analysis				
Chemical nature	Mol % in prepolymer	d/ $\mu m \pm 0{\cdot}1\,\mu m$	d/ $\mu m \pm 0{\cdot}1\,\mu m$	$2a$/ $\mu m \pm 0{\cdot}1\,\mu m$	(d-$2a$) $\mu m \pm 0{\cdot}2\,\mu m$	V_{90}/V	T_{OFF}/%
PEG 400	1·9		irregular shape and large domains			5	30
	3·3	4	3·7	2	2	7·5	5
	4·2	2·2	2·2	1·4	0·8	10	<1
	5·3	2·2	2·3	1·2	1	11	<1
	6·4	1·6	—	1·0	0·6	12	<1
PETA	3·2	2·8	3	=			
	4·9	1·7	=	=			
	7·2	1·6	=	=			

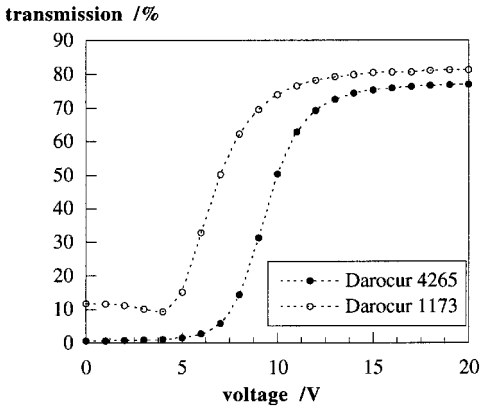

Figure 11. Dependence of nature of initiator on the voltage–transmission curves. 3 wt % of Darocur 4265 or 1173 was introduced into the prepolymer 2-EHA/8 mol % PEG400.

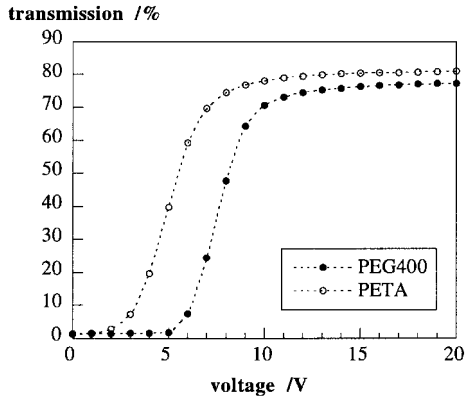

Figure 12. Dependence of nature of crosslinking agent on the voltage–transmission curves (3 mol % of PETA or PEG400 in the prepolymer).

purity of the LC-rich phase. Indeed, the gap (T-T_s) is identical for the two initial mixtures and leads to the same value of T_{INPDLC} after polymerization. This decrease in driving voltage may rather be due to weaker anchoring between the liquid crystal TL205 and the copolymer '2-EHA/PETA' compared with copolymer '2-EHA/PEG400'. This is consistent with recent studies where it has been shown that a change in the surface anchoring energy resulted in a change in the electro-optical properties. In particular, it has been reported that a better compatibility between the polymer binder and LC at the interface was responsible for a decreasing anchoring energy and switching voltage [17, 18, 19].

3.3. *Curing temperature*

The last parameter studied in this work was curing temperature. Only data obtained for highly crosslinked samples are reported here. Three films were prepared from the same initial mixture (2-EHA/6 mol % PEG400)/TL205 20:80 at different curing temperatures close to room temperature. Corresponding electro-optical curves are illustrated in figure 13. Isotropic–nematic transition temperatures $T_{IN\ (PDLC)}$ and network periodicities d of these films are reported in table 3. As

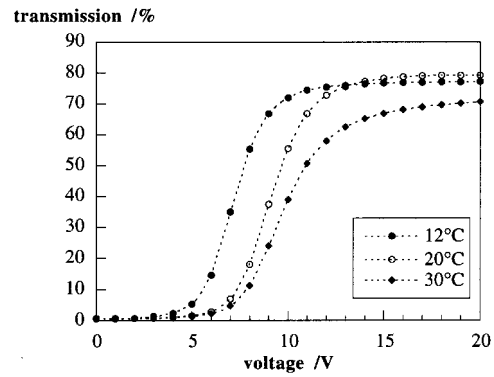

Figure 13. Voltage–transmission curves for different curing temperatures T. The prepolymer used was 6·4 mol % of PEG400 in monomer 2-EHA.

Downloaded At: 08:31 26 January 2011

Table 3. Network periodicity (d) and isotropic–nematic transition temperature $T_{IN(PDLC)}$ of (2-EHA/6 mol % PEG400)/TL205 20:80 films cured at different temperatures, T. Phase separation temperature before polymerization, T_s, of this mixture is 11°C.

Curing temperature (T)/°C	$T_{IN(PDLC)}$/°C	d/μm
12	81·7	1·5
20	81·6	1·6
30	80·7	2

already shown, when the curing process is carried out at a temperature T close to the temperature of phase separation before polymerization T_S, $T_{IN\ (PDLC)}$ is larger, which means a better purity of the LC-rich phase and thus a more efficient phase separation process (see the sample cured at 12°C). Moreover, raising the curing temperature results in a slightly larger network periodicity (d). However, one should notice that the size of the network remains small for each curing temperature ($<2\,\mu m$), which results in a weak change in the off-state transmission ($T_{OFF}<1\%$). Notice also that a more significant change in size with curing temperature was observed for a lower rate of crosslinking. Nevertheless, for a highly crosslinked PDLC, the main effect of raising the curing temperature is not on the size of the droplets, but rather on the efficiency of the phase separation process. The high efficiency of the phase separation process at low curing temperatures results in both a reduced driving voltage and a higher ON-state clarity. On the contrary, when the formation process occurs at high temperature (30°C), the pollution of the LC-rich phase strongly reduces the ON-state transmission. This latter result agrees with previous studies showing that a significant change in the refractive index of the polymer, due to the liquid crystal dissolved in it, reduces the ON-state clarity [11, 14]. Although a link between lower driving voltage and higher efficiency of the phase separation process is here experimentally advanced, this is not easy to explain. Further investigations will be necessary for a full understanding. The main result reported here is that a small gap between the curing temperature T and the temperature of phase separation before polymerization T_S leads to both high contrast and low driving voltage, which underlines once again the importance of the gap ($T - T_S$) on a film's performances.

4. Summary

To sum up, we have investigated PDLC films prepared by phase separation induced by photopolymerization. Evidence for a close relation between the formulation of the initial 'prepolymer/LC' mixture, the curing temperature and the electro-optical performances of the films is given. The determination of the purity of the PDLC LC-rich phase enables one to estimate the 'quality' of the phase separation process, while the morphology of the films allows one to visualize the organisation of the LC and polymer. We find from 'model system' investigations that a mixture composed of 80 wt % of TL205 and 20 wt % of 2-EHA leads to an efficient phase separation process. Moreover, we show that crosslinker has to be added in such a proportion that the gap between the curing temperature, T, and the temperature of phase separation before polymerization, T_S of the initial LC/prepolymer mixture is as small as possible. Indeed, the polymerization/crosslinking process must be as quick as possible in order to create a smaller morphology. The kinetics of this process are controlled by both the crosslinking agent concentration, the nature of the initiator and the UV intensity. However, this condition is not sufficient for good electro-optical performances. Indeed, driving voltage can be reduced by modifying the crosslinker's chemical structure (or the monomer's chemical structure) in order to decrease the anchoring strength at the LC/polymer interface.

Finally, we have developed an original procedure to investigate PDLC morphology. Sizes of both LC droplets ($2a$) and polymer network periodicity (d) are measured by either an FT procedure based on the analysis of microscopic images of the films or small angle light scattering experiments. This morphological investigation leads to a simple model in which LC droplets are separated by thick polymer walls whose size is given by (d-$2a$). It provides a very useful tool to compare the characteristic sizes of each film and allows the analysis of the effect of the conditions of preparation on film performances. However, this model does not take into account polymer/LC interfaces that might consist of LC in strong interaction with the polymer, as confirmed by comparing the isotropic–nematic transition enthalpy of pure LC, $\Delta H_{IN(LC)}$ with that of a PDLC film, $\Delta H_{IN(PDLC)}$. Indeed, smaller values of $\Delta H_{IN(PDLC)}$ found for all the films indicate that some LC is in strong interaction with polymer and does not undergo the isotropic–nematic transition. Evidence for the existence of these two LC populations, a 'free' one and another one strongly anchored to the polymer have already been shown [20, 21]. We find this for our systems from 30 wt % (in the case of high crosslinker concentration and high temperature) up to 90 wt % of 'free' LC. However, no obvious link between the proportion of free LC and electro-optical response was found, since the sample with the best electro-optical response contain only about 50 wt % of 'free' LC. Further information on the localization of this part of the liquid crystal at the interface between the LC domains and the polymer walls or 'trapped' in the polymer, has now to be investigated.

Downloaded At: 08:31 26 January 2011

Towards this aim, new techniques of interface investigation will have to be used.

The authors gratefully acknowledge J. Arrault, D. Bosc, F. Nallet and C. Trubert for their help and valuable discussions.

References

[1] West, J. L., 1994, *Technological Applications of Dispersions*, (Surfactant Science Series 52), pp. 349–371.
[2] See, for example, (with references therein): Doane, J. W., 1990, *Liquid Crystal Applications and Uses*, Vol 1, edited by B. Bahadur (World scientific), Chap. 14; Kitzerow, H. S., 1994, *Liq. Cryst.*, **16,** 1; Coates, D., 1995, *J. mater. Chem.*, **5,** 2063; Bouteiller, L., and LeBarny, P., 1996, *Liq. Cryst.*, **21,** 157.
[3] Grand, C., 1995, PhD thesis, Université Bordeaux I, p. 1417.
[4] *Numerical recipes. The art of scientific computing* 1986 Cambridge: Cambridge University Press.
[5] Samuels, R. J., 1971, *J. Polym. Sci. A2*, **9,** 2165.
[6] Rojstaczer, S., and Stein, R. S., 1988, *Mol. Cryst. liq. Cryst.*, **157,** 293.
[7] Stein, R. S., and Rhodes, M. B., 1960, *J. appl. Phys.*, **31,** 1873.
[8] Ding, J., and Yang, Y., 1994, *Mol. Cryst. liq. Cryst.*, **238,** 47.
[9] Ding, J., and Yang, Y., 1994, *Mol. Cryst. liq. Cryst.*, **257,** 63.
[10] Guinier, A., 1939, *Ann. Phys.*, **12,** 161.
[11] Nolan, P., Tillin, M., and Coates, D., 1992, *Mol. Cryst. liq. Cryst. Lett.*, **8,** 129.
[12] Bouteiller, L., Lebarny, P., and Martinot-Lagarde, P., 1994, *Liq. Cryst.*, **17,** 709.
[13] Smith, G. W., and Vaz, N. A., 1993, *Mol. Cryst. liq. Cryst.*, **237,** 243.
[14] Nolan, P., Tillin, M., and Coates, D., 1993, *Liq. Cryst.*, **14,** 339.
[15] Hirai, Y., Niiyama, S., Kumai H., and Gunjima, T., 1990, *SPIE* **1257,** 2.
[16] Bosc, D., Trubert, C., Vinouze, B., and Guilbert, M., 1996, *Appl. Phys. Lett.*, **68,** 2489.
[17] Nomura, H., Suzuki, S., and Atarashi, Y., 1991, *Jpn. J. appl. Phys. I*, **30,** 327.
[18] Bouteiller, L., Le Barny, P., Robin, P., and Dubois, J. C., 1994, *Proc. SID*, 195.
[19] Kim, Y. C., Lee, S. H., West, J. L., and Gelerinter, E., 1995, *J. appl. Phys.*, **77,** 1914.
[20] Hikmet, R. A. M., 1991, *Liq. Cryst.*, **9,** 405.
[21] Smith, G. W., 1995, *Mol. Cryst. liq. Cryst.*, **241,** 37.

Downloaded At: 08:31 26 January 2011